Commun Nonlinear Sci Numer Simulat 32 (2016) 234–240

Contents lists available at ScienceDirect

Commun Nonlinear Sci Numer Simulat

journal homepage: www.elsevier.com/locate/cnsns

Ergodicity of a singly-thermostated harmonic oscillator

William Graham Hoover [a,*], Julien Clinton Sprott [b], Carol Griswold Hoover [a]

[a] Ruby Valley Research Institute, Highway Contract 60, Box 601 Ruby Valley, NV 89833, USA
[b] Department of Physics, University of Wisconsin–Madison, WI 53706, USA

ARTICLE INFO

Article history:
Received 25 June 2015
Revised 22 August 2015
Accepted 25 August 2015
Available online 1 September 2015

PACS:
0.05

Keywords:
Ergodicity
Chaos
Algorithms
Dynamical systems

ABSTRACT

Although Nosé's thermostated mechanics is formally consistent with Gibbs' canonical ensemble, the thermostated Nosé–Hoover (harmonic) oscillator, with its mean kinetic temperature controlled, is far from ergodic. Much of its phase space is occupied by regular conservative tori. Oscillator ergodicity has previously been achieved by controlling two oscillator moments with *two* thermostat variables. Here we use computerized searches in conjunction with visualization to find *singly*-thermostated motion equations for the oscillator which are consistent with Gibbs' canonical distribution. Such models are the simplest able to bridge the gap between Gibbs' statistical ensembles and Newtonian single-particle dynamics.

1. Ergodicity of the equations of motion

Gibbs' statistical mechanics is based on summing contributions from ensembles of similar systems. His *microcanonical* ensemble includes all the states of a given system which have the same energy. These energy states are accessible to a single "ergodic" system obeying Newtonian mechanics [1]. A periodic hard-disk or hard-sphere fluid is the usual example. Comparisons of Monte Carlo microcanonical-ensemble averages with molecular dynamics dynamical averages have confirmed this equivalence, even for small systems of just a few particles [2].

Certainly Boltzmann and Gibbs both realized that *all* states need to be accessible to the dynamics in order for the dynamical and phase averages to correspond. The Ehrenfests had a practical definition of "quasiergodicity". They used the word to indicate that the dynamics eventually comes "arbitrarily close" to all states. Their idea expresses very well our own view of what we call "ergodicity" in the present work.

Gibbs' *canonical* ensemble sums Boltzmann-weighted contributions from *all* energy states. The underlying idea is that the system of interest is weakly coupled to a heat reservoir with an ideal-gas density of states characteristic of a fixed kinetic temperature T. Nosé [3,4] developed a dynamics consistent with the canonical distribution by including a "time-scaling" variable s and its conjugate momentum p_s in the equations of motion. The new momentum p_s acts as a thermostat variable capable of exchanging energy between the system and a heat reservoir at temperature T.

Hoover showed that a harmonic oscillator thermostated in this way is not at all ergodic [5]. That is, there is no initial condition from which the oscillator is able to access *all* of its phase-space states. Instead, this thermostated oscillator has a nonergodic highly-complicated multi-part phase-space structure [6]. There are infinitely-many regular nonchaotic orbits embedded in a

* Corresponding author. Tel.: +017757792266.
E-mail address: hooverwilliam@yahoo.com (W.G. Hoover).

http://dx.doi.org/10.1016/j.cnsns.2015.08.020
1007-5704/

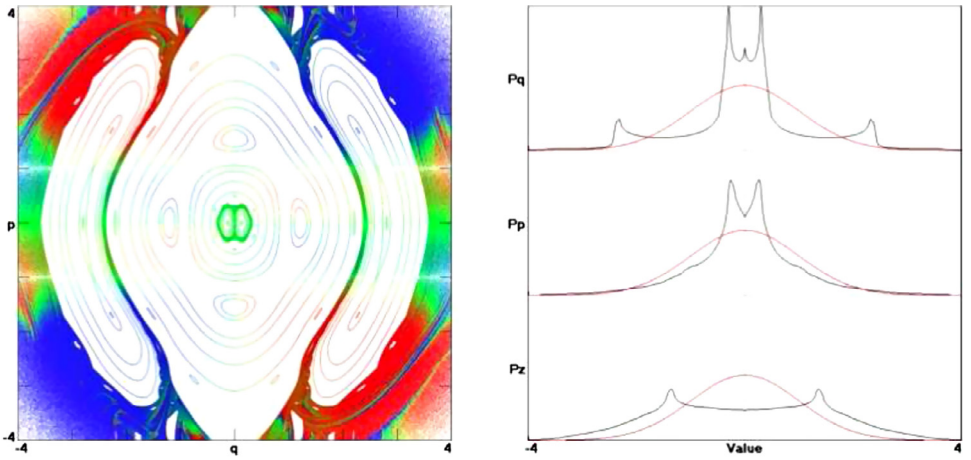

Fig. 1. This Nosé–Hoover oscillator phase-space section corresponds to the plane $\zeta = 0$. The coloring reflects the local value of the instantaneous Lyapunov exponent at each $(q, p, 0)$ point, with red least stable and blue most. The distributions of $\{q, p, \zeta\}$ in the chaotic sea are compared to Gibbs' Gaussian distributions at the right. The white space indicates nonchaotic regions filled with regular nested tori, some of which are shown. In the chaotic sea $\lambda_1 = \langle \lambda_1(t) \rangle = 0.0139$. (For interpretation of the references to color in this figure legend, the reader is referred to the web version of this article).

single chaotic sea. Where "chaos" controls the motion two closeby points, $r_1(t)$ and $r_2(t)$, tend to separate from one another exponentially fast, either forward or backward in time. Such a motion is said to be "Lyapunov unstable". The averaged separation rate is described by the largest Lyapunov exponent, λ_1:

$$\delta \equiv |r_2 - r_1| \simeq e^{\lambda_1 t};\ \lambda_1 \equiv \langle \lambda_1(t) \rangle .$$

The time-averaged Lyapunov exponent λ_1 is computed as an average of the instantaneous local Lyapunov exponent, $\lambda_1(t)$. The local value is only rarely zero, even on conservative tori, where the long-time averages vanish. We illustrate $\lambda_1(t)$ for the Nosé–Hoover oscillator in Fig. 1. We choose the simplest equations of motion,

$$\{\dot{q} = p;\ \dot{p} = -q - \zeta p;\ \dot{\zeta} = p^2 - 1\}\ [\mathrm{NH}].$$

They are time-reversible: any time-ordered sequence $\{+q, +p, +\zeta\}$ satisfying the motion equations has a time-reversed backward twin, $\{+q, -p, -\zeta\}$ satisfying the same equations. The Nosé–Hoover oscillator in $\{q, p, \zeta\}$ space is an improved and simplified version of Nosé's dynamics, which occupies a four-dimensional $\{q, p, s, p_s\}$ space [5,6].

For this Nosé–Hoover oscillator we have computed the local Lyapunov exponent on a grid of about a million points by the simple expedient of integrating backward in time and then forward, for a time of 100 in both directions. The "reversed" trajectory going forward in time can be compared to a nearby constrained "satellite" trajectory. We compute the instantaneous value of the time-dependent Lyapunov exponent just as the $\zeta = 0$ plane is crossed. In the figure red corresponds to the most positive exponent value and blue to the most negative. Within the chaotic sea the largest (time-averaged) Lyapunov exponent is 0.013_9. See Reference 6 for details.

Outside the chaotic sea lie an infinite number of regular orbits. All have a largest time-averaged Lyapunov exponent (and also a smallest) of zero. Because the oscillator is prototypical of systems with smooth minima in their energy surfaces a considerable effort has been made to find motion equations providing Gibbs' canonical distribution for it [7–18].

2. Feedback control of oscillator moments

For simplicity we choose units of force, mass, time, and temperature corresponding to choosing the oscillator force constant, mass, angular velocity, and Boltzmann's constant all equal to unity. In these units and without any thermostating the oscillator motion equation is $\ddot{q} = \dot{p} = -q$. Because distribution functions for the oscillator's displacement and momentum can be described in terms of their moments $\langle q^{2m} p^{2n} \rangle$, it was natural to control oscillator force and velocity moments with feedback variables such as ζ and ξ:

$$\{\dot{q} = p - \xi q;\ \dot{p} = -q - \zeta p\}.$$

The time dependence of the friction coefficients $\zeta(t)$ and $\xi(t)$ can be arranged so as to control one or more of the oscillator moments:

$$\dot{\zeta} = (p^2/T) - 1 \to \langle p^2 \rangle \equiv T;\ \dot{\xi} = (q^4/T^2) - 3(q^2/T) \to \langle q^4 \rangle \equiv 3T \langle q^2 \rangle\ \ldots .$$

Bulgac and Kusnezov, along with their coworkers Bauer and Ju [15,16], considered a variety of simple systems and concluded that *cubic* contributions to the control equations, such as those in the [HH] and [JB] equations below, were especially useful in promoting chaos and ergodicity.

Over thirty years dozens of investigators explored the ergodicity of thermostated oscillators [7–18]. Three successful models, the Hoover–Holian [13], Ju–Bulgac [15], and Martyna–Klein–Tuckerman models [17] resulted. With all of the thermostat relaxation times set equal to unity, these models have the following forms:

$$\dot q = p;\ \dot p = -q - \zeta p - (\xi p^3/T);\ \dot\zeta = (p^2/T) - 1;\ \dot\xi = (p^4/T^2) - 3(p^2/T);\ \text{[HH]}$$
$$\dot q = p;\ \dot p = -q - \zeta^3 p - (\xi p^3/T);\ \dot\zeta = (p^2/T) - 1;\ \dot\xi = (p^4/T^2) - 3(p^2/T);\ \text{[JB]}$$
$$\dot q = p;\ \dot p = -q - \zeta p;\ \dot\zeta = (p^2/T) - 1 - \xi\zeta;\ \dot\xi = \zeta^2 - 1.\ \text{[MKT]}$$

In all three cases the phase-space continuity equation,

$$(\partial f/\partial t) = -(\partial f\dot q/\partial q) - (\partial f\dot p/\partial p) - (\partial f\dot\zeta/\partial\zeta) - (\partial f\dot\xi/\partial\xi).$$

shows that the motion equations are consistent with Gibbs' canonical distribution for the (q, p) coordinate-momentum pair:

$$f(q, p) = e^{-q^2/2T}e^{-p^2/2T}/(2\pi T).$$

The distributions of the control variables ζ and ξ are likewise Gaussians:

$$f_{HH} = f_{MKT} \propto e^{-\zeta^2/2}e^{-\xi^2/2};\ f_{JB} \propto e^{-\zeta^4/4}e^{-\xi^2/2}.$$

If the dynamics is ergodic, filling out the full distributions, these models reproduce Gibbs' canonical distribution.

Although there are no *theoretical* proofs that these dynamics obey the phase-space distributions and relationships there is by now abundant *numerical* evidence that the three two-thermostat approaches given above *are* ergodic [19]. Recent work, particularly that of Patra and Bhattacharya [20,21], led us to search for even simpler models, with three equations rather than four, for thermostated oscillators. We describe our own quite novel and successful findings next.

3. Singly-thermostated ergodic oscillator models

A first look at the possibility of thermostating an oscillator with a single friction coefficient corresponds to a variety of separate models. We consider two of them here. Both include cubic functions as suggested by Bulgac, Kusnezov, Ju, and Bauer. The first oscillator model controls the fluctuation of the kinetic energy:

$$\dot q = +p;\ \dot p = -q - \alpha(\zeta^3 p^3/T);\ \dot\zeta = \alpha[(p^2/T)^2 - 3(p^2/T)].$$

The second controls the fluctuation of the force:

$$\dot q = +p - \beta\zeta^3 q;\ \dot p = -q;\ \dot\zeta = \beta[(q^2/T) - 1].$$

Neither of these approaches is successful. In Figs. 2 and 3 we show the chaotic seas corresponding to these two models with first α and then β equal to unity. In both cases we choose unit temperature, $T = 1$. We plot (q, p) points whenever the friction coefficient ζ changes sign. These models both contain holes in the sea filled with regular toroidal regions. The one-dimensional distribution functions shown at the right of these figures give an alternative view of the models' inability to describe Gibbs' canonical distribution. Both of these single-thermostat models are failures. In addition to plotting cross sections and probability

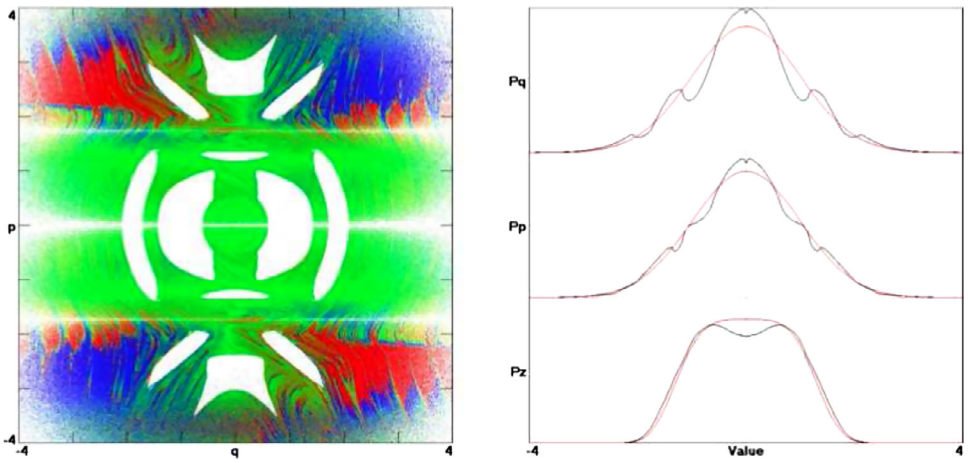

Fig. 2. Single-thermostat cubic control enforcing the fourth-moment condition, $\langle p^4\rangle = 3\langle p^2\rangle$ with α and T both equal to unity and $\beta = 0$. These choices show large gaps in the cross section where the time-averaged Lyapunov exponent vanishes. The probability densities within the chaotic sea are shown at the right. The initial condition used here and in all succeeding figures to access the chaotic sea is $(q, p, \zeta) = (0, 5, 0)$. The three horizontal nullclines at $\{p = -\sqrt{3}, 0, +\sqrt{3}\}$ reflect the vanishing of the phase-space velocity component normal to the $\zeta = 0$ plane. $\lambda_1 = 0.1108$ in the chaotic sea.

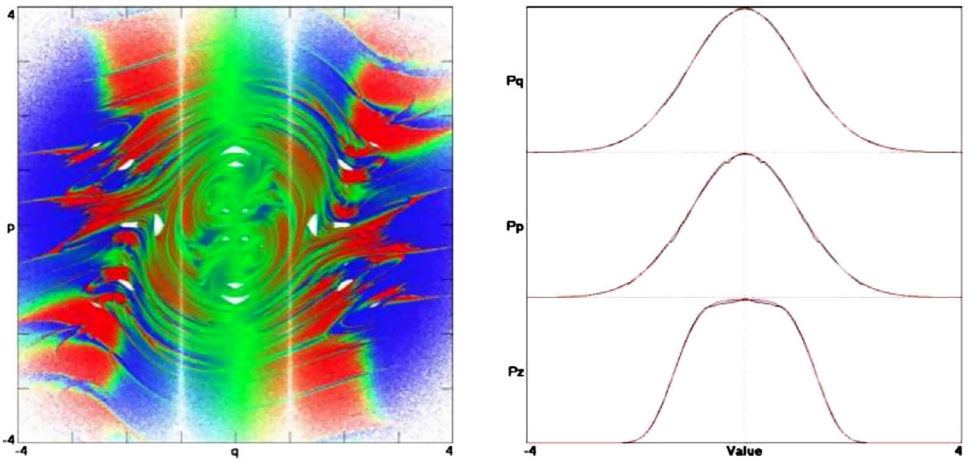

Fig. 3. Single-thermostat cubic control enforcing the second moment condition $\langle q^2 \rangle = 1$ with β and T set equal to unity and $\alpha = 0$. These choices show the presence of at least twenty gaps (or "holes") in the cross section where the friction coefficient ζ vanishes. The one-dimensional probability densities within the chaotic sea are shown at the right along with the Gibbs' distributions from the canonical ensemble. $\lambda_1 = 0.0905$ in the chaotic sea.

densities one can evaluate the likelihood of deviations from Gibbs' values as measured by the χ^2 statistic described in Wikipedia, *Numerical Recipes*, and many other texts.

At least in retrospect it is natural to consider the possibility that a *single* friction coefficient ζ might somehow control *two* moments simultaneously, rather than just one. For example, consider simultaneous control of *fluctuations* in *both* the force $\simeq \langle q^2 \rangle$ and the kinetic energy $\simeq \langle p^4 - 3p^2T \rangle$:

$$\dot{q} = +p - \beta\zeta^3 q; \; \dot{p} = -q - \alpha(\zeta^3 p^3/T);$$
$$\dot{\zeta} = \beta[(q^2/T) - 1] + \alpha[(p^2/T)^2 - 3(p^2/T)] \; [\text{HS}].$$

Our numerical work indicates that this [HS] (Hoover–Sprott) idea has merit. With *two* free parameters (α, β) there are an infinite number of models which could be tested against the predictions of Gibbs' canonical ensemble. This variety could be extended further by including one or more relaxation times. To choose among the combinations of $\{\alpha, \beta\}$ it is convenient to use computerized searches, either seeking minimum deviations with Monte Carlo searches [22] or by choosing minima from grid-based arrays of (α, β) results.

We use standard Runge–Kutta integration methods throughout this work, fourth-order and fifth-order as well as two types of "adaptive" integrators. In the adaptive cases the timestep dt is doubled if the error is "small" (typically 10^{-16}) and halved if the error is "large" (typically 10^{-12}). The error estimate compares either fourth-order and fifth-order results with the same timestep dt or two fourth-order results with dt and $dt/2$. There are no significant differences in the conclusions reached with any of these several methods. We carried out independent calculations in Nevada and in Wisconsin.

With either two-parameter approach, the computation of moments is straightforward. Optimizing the dynamics so as to seek out the Gibbs distribution can be accomplished by evaluating either [1] moments of the distribution $f(q, p)$ or [2] values of the distribution itself. To follow the first approach we minimized the summed-up squared deviations of the first five nonvanishing Gibbsian moments:

$$\sigma^2 \equiv [(q^4/T^2) - 3] + [(q^2p^2/T^2) - 1] + [(p^4/T^2) - 3] + [(q^2/T) - 1] + [(p^2/T) - 1].$$

We evaluated σ^2 for thousands of runs. Each used 100 million timesteps for a particular pair of candidate values (α, β). Time-averaged values of σ^2 suggest the range $0.25 < \alpha < 0.65$ with $1 < \alpha + \beta < 1.1$. Figs. 4–6 show three typical cross-sectional plots of $\{q, p\}$ sections selected in this way. Fig. 4, with $(\alpha, \beta) = (0.411, 0.689)$, shows 26 noticeable "holes" with a total measure near one percent of the total. The figure also illustrates the figure-eight-shaped nullcline where trajectories move parallel to the $\zeta = 0$ plane with $\dot{\zeta} \equiv 0$;

$$\beta[(q^2/T) - 1] + \alpha[(p^2/T)^2 - 3(p^2/T)] \equiv 0.$$

Despite all the holes indicating nested tori the distribution functions and their first several moments are close to the Gibbsian ergodic values. Evidently there is no real substitute for looking at the sections themselves.

Fig. 5, with $(\alpha, \beta) = (0.354, 0.746)$, likewise provides "reasonable" distributions and moments, but has four holes where nested tori penetrate the cross section. Figs. 4 and 5 hint at the extensive zoo of topologies hidden in the (α, β) plane. There are in addition patches of values which evidently correspond to ergodicity. Two examples which we think are likely ergodic are:

$$(0.273, 0.827) \text{ and } (0.274, 0.826).$$

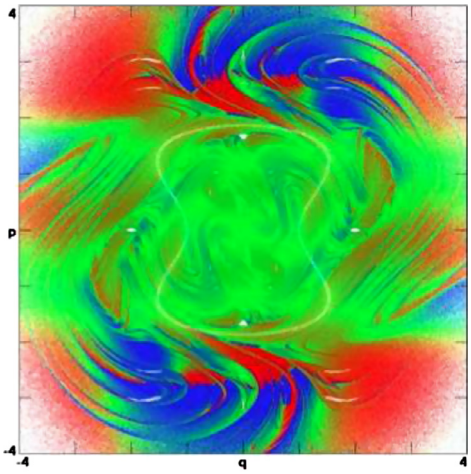

Fig. 4. $(\alpha, \beta) = (0.411, 0.689)$. A close inspection shows 26 prominent "holes" with a total measure less than one-half percent of the total. The figure also illustrates the typical figure-eight-shaped nullcline where the trajectory motion is parallel to the $\zeta = 0$ plane. Because the deviations of the various one-dimensional probability densities are visually indistinguishable from Gibbs' canonical distributions none of them is shown in Figs. 4–6. Here $\lambda_1 = 0.1621$ in the chaotic sea.

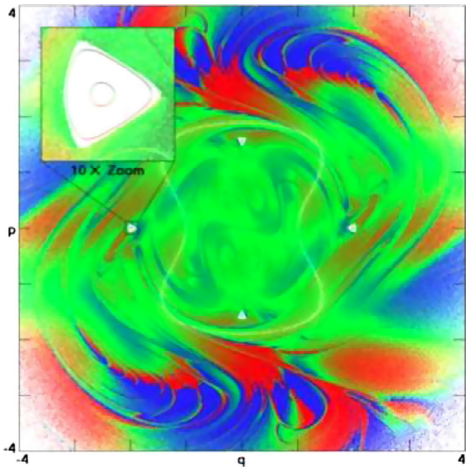

Fig. 5. $(\alpha, \beta) = (0.354, 0.746)$ likewise provides "reasonable" distributions and moments, but has four holes where nested tori penetrate the cross section. The tenfold "zoom" of one hole shows their roughly triangular shape. Here $\lambda_1 = 0.1525$ in the chaotic sea.

The first of these is plotted in Fig. 6. It has no noticeable "holes", indicating ergodicity within an accuracy of about one part per hundred thousand. Again the Figure-Eight-Shaped white space indicates the nullcline, which depends weakly on the precise value of the ratio (α/β).

One can only search for "holes" in sections visually. An example, which we thought to be ergodic after a cursory inspection, is the combination $(\alpha, \beta) = (0.495, 0.555)$, not shown here because visualizing the holes requires magnification. A close inspection of the $\zeta = 0$ section reveals 36 tiny holes (!) corresponding to a single thin set of nested tori, including two near $(q, p) = (\pm 1.5, 0.0)$. These tori cross the $\zeta = 0$ plane in 36 separate places.

Because the numerical value of the summed squared-moment errors depends upon both the initial conditions and the length of the trajectories a reasonable procedure is to investigate visually, as second and third criteria for ergodicity, the distributions themselves as well as their (q, p) cross sections. Such inspections reveal the (α, β) pairs most promising from the standpoint of ergodicity. The distributions found for the cross sections of the Figs. 1–3 are included in those figures. From the visual standpoint such histograms show no significant deviations from the ergodic distribution in the data displayed for Figs. 4 and 5, despite the clear nonergodicity seen in the cross sections. Our results suggest overall that a *visual* inspection of two-dimensional cross sections is the most reliable way to identify ergodicity in these three-dimensional dynamical systems.

An alternative method for evaluating ergodicity is to compute the probability that a measured distribution of data points, such as $\{q_i\}$ or $\{p_i\}$ or $\{\zeta_i\}$ comes from the expected Gaussian distribution of such points. Comparing the probabilities for the three choices demonstrates the accuracy of such a test. So long as the sampling bins contain many points the mean-squared

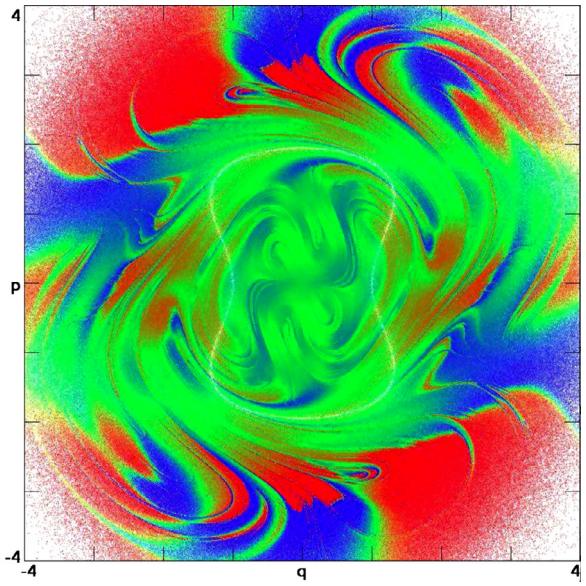

Fig. 6. $(\alpha, \beta) = (0.273, 0.827)$ is just one of an infinite number of combinations that is apparently ergodic. $\lambda_1 = 0.1450$.

deviation of the bin populations should be approximately equal to Gibbs' value. Such tests implementing χ^2 criteria can serve as useful indicators for deviations from ergodicity. In any doubtful case visual inspection is the only reliable criterion.

4. Phase-space density flows

An apparent alternative to solving the motion equations $\{\dot{q}, \dot{p}, \dot{\zeta}\} = \nu$ for a specimen oscillator is the solution of Liouville's continuity equation, $\dot{f}/f = -\nabla \cdot \nu$, so as to study the details of the convergence (or lack of it) to Gibbs' canonical distribution. We briefly considered this approach and developed a straightforward finite-difference program simulating the three-dimensional flow of the probability density $f(q, p, \zeta, t)$. This program quickly led to negative densities. A conservative approach, passing probabilities between adjacent cells, can be implemented with a swarm of N moving particles, all of equal probability. The instantaneous summed-up density of these particles at any point in phase space can be made continuous and twice-differentiable by defining and computing a smooth-particle density. This idea is simplest to implement using Lucy's weight function [23] $w(r < h)$ with a range h of order two or three times the nearest-neighbor particle spacing:

$$f(q, p, \zeta) \equiv \sum_i^N w(r - r_i); \; w(z = r/h < 1) \propto (1 + 3z)(1 - z)^3.$$

We explored this idea using an initial condition $f(0 < q, p, \zeta < 1) \equiv 1$ and noticed that such a localized initial value requires several Lyapunov times to smooth out. The particulate basis of the density guarantees that there is no tendency for this solution of the Liouville flow to stabilize. The time-reversible nature of the flow guarantees that a smooth stationary solution can only be obtained by adding in a time-averaging step. A detailed investigation of these ideas is likely worthwhile in that the compact three-dimensional nature of these flows makes visualization easy.

5. Summary

It appears highly likely that a single thermostat variable *is* enough to provide Gibbs' canonical distribution for a thermostated harmonic oscillator. This question has stimulated a relatively complex and varied literature over a 30-year period. The mathematicians are content to prove nonergodicity [24]. The computational physicists, ourselves included, have been prone to give up on the possibility of ergodicity with a single thermostat variable [25]. Thus our finding that one thermostat *is* enough was a pleasant surprise. The (α, β) model detailed here seems likely to be the simplest smoothly deterministic, ergodic, time-reversible, and chaotic system for which the phase-space distribution is exactly known.

Acknowledgment

Bill and Carol Hoover particularly appreciate a recent extended conversation with John Ramshaw concerning the feasibility of ergodicity studies. We have also all benefited from experience gleaned from Puneet Patra's and Baidurya Bhattacharya's investigations of the ergodicity of the Martyna–Klein–Tuckerman and their own multi-moment [PB] oscillator models.

References

[1] Lebowitz JL, Penrose O. Modern ergodic theory. Phys Today February 1973:1–7.
[2] Hoover WG, Alder BJ. Studies in molecular dynamics. iv. the pressure, collision rate, and their number dependence for hard disks. J Chem Phys 1967;46:686–91.
[3] Nosé S. A molecular dynamics method for simulations in the canonical ensemble. Mol Phys 1984;52:255–68.
[4] Nosé S. A unified formulation of the constant temperature molecular dynamics methods. J Chem Phys 1984;81:511–19.
[5] Hoover WG. Canonical dynamics: equilibrium phase-space distributions. Phys Rev A 1985;31:1695–7.
[6] Posch HA, Hoover WG, Vesely FJ. Canonical dynamics of the Nosé oscillator: stability, order, and chaos. Phys Rev A 1986;33:4253–65.
[7] Hoover WG. Molecular dynamics. Lecture notes in physics, vol. 258. Berlin: Springer-Verlag; 1986. p. 30.
[8] Dettmann CP, Morriss GP. Hamiltonian reformulation and pairing of Lyapunov exponents for Nosé-Hoover dynamics. Phys Rev E 1997;55:3693–6. See also Reference 9.
[9] Bond D, Leimkuhler BJ, Laird BB. The Nosé–Poincaré method for constant temperature molecular dynamics. J Comput Phys 1999;151:114–34. See also Reference 8.
[10] Braga C, Travis KP. A configurational temperature Nosé–Hoover thermostat. J Chem Phys 2005;123:134101.
[11] Brańka AC, Kowalik M, Wojciechowski KW. Generalization of the Nosé-Hoover approach. J Chem Phys 2003;119:1929–36.
[12] Hamilton IP. Modified Nosé–Hoover equation for a one-dimensional oscillator: enforcement of the virial theorem. Phys Rev A 1990;42:7467–80.
[13] Hoover WG, Holian BL. Kinetic moments method for the canonical ensemble distribution. Phys Lett A 1996;211:253–7.
[14] Jellinek J, Berry RS. Generalization of Nosé's isothermal molecular dynamics: necessary and sufficient conditions of dynamical simulations of statistical ensembles. Phys Rev A 1989;40:2816–18.
[15] Ju N, Bulgac A. Finite-temperature properties of sodium clusters. Phys Rev B 1993;48:2721–32.
[16] Kusnezov D, Bulgac A, Bauer W. Canonical ensembles from chaos. Ann Phys 1990;204:155–85.
[17] Martyna GJ, Klein ML, Tuckerman M. Nosé–Hoover chains: the canonical ensemble *via* continuous dynamics. J Chem Phys 1992;97:2635–43.
[18] Winkler RG. Extended-phase-space isothermal molecular dynamics: canonical harmonic oscillator. Phys Rev A 1992;45:2250–5.
[19] Hoover WG, Hoover CG. Ergodicity of a time-reversibly thermostated harmonic oscillator and the 2014 Ian Snook Prize. Comput Methods Sci Technol 2014;20:87–92.
[20] Patra PK, Bhattacharya B. Non-ergodicity of Nosé–Hoover chain thermostat in computationally achievable time. Phys Rev E 2014;90:043304.
[21] Hoover WG, Sprott JC, Patra PK. Ergodic time-reversible chaos for Gibbs' canonical oscillator. Phys Lett A (in press).
[22] Sprott JC. Some simple chaotic flows. Phys Rev E 1994;50:R647–50.
[23] Hoover WG, Hoover CG. Smooth-particle mechanics, the state of the art. Advanced series in nonlinear dynamics. Singapore: World Scientic; 2006.
[24] Legoll F, Luskin M, Moeckel R. Nonergodicity of the Nosé-Hoover thermostatted harmonic oscillator. Arch Ration Mech Anal 2007;3(184):449–63.
[25] Watanabe H, Kobayashi H. Ergodicity of a thermostat family of the Nosé–Hoover type. Phys Rev E 2007;75:040102R.